Available online at www.sciencedirect.com
SCIENCE DIRECT®
Atmospheric Environment 39 (2005) 813–821
ATMOSPHERIC ENVIRONMENT
www.elsevier.com/locate/atmosenv

Emission inventory of eight elements, Fe, Al, K, Mg, Mn, Na, Ca and Ti, in dust source region of East Asia

Jie Xuan*

Environment Science Center, Peking University, Beijing 100871, PR China

Received 6 July 2004; received in revised form 8 October 2004; accepted 22 October 2004

Abstract

Based on calculation of the emission rate of the atmospheric mineral dust and the data of elemental contents in surface soils, this paper calculates the emission inventory of eight main elements of the atmospheric dust, Fe, Al, K, Mg, Mn, Na, Ca and Ti, in the dust source region of East Asia. As the dust sources in both Northern China and the Southern Mongolia are of three types and, in each of the six source type areas, surface soils are relatively uniform in soil types and soil texture, a simple method to calculate the emission of an element in one source type area is proposed by multiplying the total emission of the dust PM_{10} and PM_{50} in the source type area with the mean percentage content of the element in surface soils of the area. Comparison of our calculation of the total Fe emission in the source region of East Asia with the total Fe deposition to the North Pacific Ocean, measured and calculated by previous authors, shows very good agreement. This general method can also be used for the emission calculation of any other element.

Keywords: Atmospheric dust; Dust emission; Element emission; Dust sources; East Asia

1. Introduction

In studying the atmospheric mineral dust, most researches are aimed on the radiative impacts of the dust on global climate, while many researchers are involved in the chemical or elemental composition of the dust. For example, chemical and elemental analyses of the dust particles provide us the information of the dust origination or dust sources and transportation routes (Nagoya University, 1995; Choi et al., 2001; Ma et al., 2004; Topping et al., 2004). The analyses can also be used for identifying oil field fires (Tazaki et al., 2004) and other anthropogenic pollutants from natural dust (Senaratne and Shooter, 2004). The deposition of the atmospheric mineral dust provides iron (Fe) to the global ocean, which regulates the phytoplankton growth and, consequently, the oceanic eco-system (Gao et al., 2001; 2003). In general, we have to know the concentration of suspended particles in the air and their chemical contents before simulating their physical and chemical effects on the atmosphere. It is essential to calculate the emission rates of these chemicals and elements in a specific dust source region. In particular, dust sources in East Asia are among the main world dust sources, but rather different from the others. The difference comes from not only its high latitude and high elevation but also from the characteristics in climate, morphology, soil texture, topography and dust storm activities (Xuan and Sokolik, 2002; Xuan et al., 2004). For example, the peak of the dust emission (frequent dust storms) appears in spring in the source region of East Asia (Littmann, 1991; Middleton, 1991), while for Sahara Desert and most

*Corresponding author. Tel.:/fax: +86 10 62871784.
E-mail addresses: jiexuan@pku.edu.cn, jiexuan46@yahoo.com (J. Xuan).

1352-2310/$ - see front matter © 2004 Elsevier Ltd. All rights reserved.
doi:10.1016/j.atmosenv.2004.10.029

other sources, the peak appears in summer (Prospero et al., 2002).

In Section 2 of this paper, some general features of the dust source region in East Asia are briefly described with the contour map of the annual dust emission rate for PM_{10}, dust particles smaller than 10 μm. The inventory of the annual and seasonal emissions of dust PM_{10} and PM_{50} in different parts of the dust source region is listed in a table. In Section 3, by using the maps of the content grades of 56 elements in surface soils of China (Zheng, 1994) and supposing an accordant correlation between the elemental contents and soil types or textures for the whole Mongolian Plateau, the seasonal and annual elemental emission rate of the eight elements in dust PM_{10} and PM_{50} is calculated in the source region of East Asia, they are: Ferrum (Fe), Aluminum (Al), Kalium (K), Magnesium (Mg), Manganese (Mn), Sodium (Na), Calcium (Ca) and Titanium (Ti). The eight elements have been proved among main elements of Asian dust (Nagoya University, 1995; Choi et al., 2001). Eight contour maps of the annual elemental emission rate are drawn, all of which show similar distribution pattern with that of the emission rate of dust PM_{10}. As the dust sources in both Northern China and the Southern Mongolia are of three types and, in each of the six source type areas, surface soils are relatively uniform in soil types and soil texture, a simple method to calculate the emission of an element in one source type area is proposed by multiplying the total emission of the dust PM_{10} and PM_{50} in the source type area with the mean percentage content of the element in surface soils of the area. The method can also be used for the emission calculation of the rest 48 elements. Comparison of our calculation of the total Fe emission from the dust source region in East Asia with the measurement and calculation of the total Fe deposition to the North Pacific Ocean by previous authors (Gao et al., 2001) shows good agreement.

2. Dust source region in East Asia and the emission of PM_{10} and PM_{50}

Fig. 1 shows the dust source region in East Asia, which consists of deserts and gobi-deserts in Northern China and Southern Mongolia. The dust source region comprises two parts or systems: (i) Mongolian Plateau system, including deserts and gobi-deserts on the Mongolian Plateau and its south extension—the Ordos Plateau and Alxa Plateau; and (ii) Tarim Basin system, including deserts and gobi-deserts in the Tarim Basin, Junggar Basin and their east vicinity (Xuan et al., 2004). The two systems have commonalities as well as important differences in characteristics of the palaeo-geography, topography, morphology (the distribution pattern of deserts and gobis, with or without a large area of downwind loess deposition), soil texture, climate and, especially, the dust storm meteorology. There are three types of dust sources in the region, roughly distributed from east to west (Fig. 1):

Type 1: deserts in dry agricultural areas,

Type 2: deserts and gobi-deserts on flat plateaus, and

Type 3: deserts and gobi-deserts in topographical lows (Xuan and Sokolik, 2002; Xuan et al., 2004).

Type 3 source area in China coincides with the Tarim Basin system, while the Mongolian Plateau system covers the other five source-type areas. Far from the oceans, the climate is very dry and continental, and the rare precipitation occurs mostly in summer season. In late winter and spring, when the strong frontal winds—the cold waves from Siberia—frequently flow through the vast area, a huge amount of dust is lifted from the

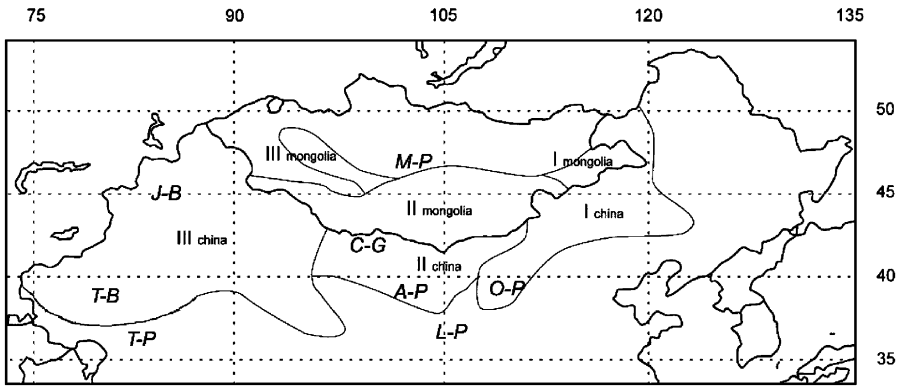

Fig. 1. Dust region in East Asia, showing three source types in China and Mongolia. Geographical abbreviations mark the following landscapes: M-P: Mongolian Plateau, covering whole Mongolia and a south narrow strip inside China; O-P: Ordos Plateau; A-P: Alxa Plateau; L-P: Loess Plateau; C-G: Central Gobi-desert; J-B: Junggar Basin, where lies the Gurbantunggut Desert; T-B: Tarim Basin, where lies the Taklimakan Desert; T-P: Tibetan Plateau.

driest surfaces, forming severe dust storms. These dust storms are moving southeast along with the surface prevailing winds. For millions of years, dust deposition of these dust storms has formed the vast Loess Plateau southeast of the Mongolian Plateau. Smaller dust particles are often up-lifted to a few kilometers high, traveling eastward, over the North-Pacific Ocean and reaching North America.

This paper suggests, with a little arbitrariness, that the emission rate of dust PM_{50}, Q_{50}, is quantitatively related with the gravitational deposition to local downwind area of dust sources while the emission rate of dust PM_{10}, Q_{10}, can be considered mostly contributing to the distant transportation as meteorological observation in Korean Peninsula which always records an elevated high concentration of PM_{10} during spring dust event periods (Choi et al., 2001). Table 1 lists the acreage of the six source-type areas and the inventory of the dust emission for PM_{10} and PM_{50}, both annually and seasonally, which we calculated with two US EPA formulas. There are totally 131 grid points for the calculation, most of which are $2.5^\circ \times 2.5^\circ$ apart except for those close to the borders or the coastline. Most of the calculation technics can be found from Xuan (1999), Xuan et al. (2000), Xuan and Sokolik (2002), and Xuan et al. (2004) except for the seasonal dust emission rates in Mongolia, the calculation technics of which are briefly described as follows: the main difficulty is in the lack of data, which we solved in the following way. The Sina–Mongolian border lies across the Mongolian Plateau from west to east. North of the border, Mongolia takes most part of the plateau, while China takes its south strip named Inner-Mongolia Plateau. We chose 10 grid points in Chinese side and very close to the border with Mongolia, and calculated the average seasonal variation proportion in dust emission rates at these grid points. Supposing an accordant seasonal variation for the whole Mongolian Plateau, we then divided the annual dust emission rate at a grid point in Mongolia, which we had calculated before, into the four seasons in a unique proportion—the average proportion calculated at the 10 points on the Inner-Mongolia Plateau.

As example, Fig. 2 shows the contour map of the annual dust emission rate Q_{10} in Northern China and Mongolia. It can be seen from the contours that the dust emission rate Q_{10} is generally increased from north to south on the Mongolian Plateau along with rapid decrease in precipitation and increase in the aridity. While in other parts of the dust source region in East Asia, the emission rate is increased from east to west, getting closer and closer to the center of the vast Eurasian Continent. Also, in the figure, there are two strong dust emission centers circled by the contours of $Q_{10} = 10^{-1} \times 10^6\,\mathrm{t\,ha^{-1}\,yr^{-1}}$: one in the Tarim Basin, i.e., the Taklimakan Desert, while the other is the Central gobi-desert on the south Mongolian Plateau. It can be seen from the contour map that the dust source region in East Asia further extends west and southwest,

Table 1
Areas and emissions of PM_{10} and PM_{50} of the six source type areas

	Type 1 (Mongolia)	Type 2 (Mongolia)	Type 3 (Mongolia)	Type 1 (China)	Type 2 (China)	Type 3 (China)	Total source region
Area ($10^4\,km^2$)	12.3	59.4	12.3	78.7	61.2	105.3	329.2
$PM_{10,\ annual}$ (10^6 ton)	0.026	2.00	0.027	0.092	2.90	5.40	10.44
$PM_{10,\ spring}$ (10^6 ton)	0.012	0.94	0.013	0.070	1.50	3.40	5.93
$PM_{10,\ summer}$ (10^6 ton)	0.003	0.20	0.003	0.002	0.30	0.20	0.72
$PM_{10,\ autumn}$ (10^6 ton)	0.002	0.18	0.002	0.010	0.30	1.50	1.99
$PM_{10,\ winter}$ (winter)	0.009	0.68	0.009	0.010	0.80	0.30	1.80
$PM_{50,\ annual}$ (10^6 ton)	0.037	8.60	0.049	0.50	13.20	28.90	51.29
$PM_{50,\ spring}$ (10^6 ton)	0.018	4.13	0.024	0.26	4.68	18.60	27.70
$PM_{50,\ summer}$ (10^6 ton)	0.005	1.12	0.006	0.03	1.22	1.70	4.08
$PM_{50,\ autumn}$ (10^6 ton)	0.003	0.77	0.004	0.12	1.70	7.52	10.12
$PM_{50,\ winter}$ (10^6 ton)	0.011	2.58	0.015	0.09	5.60	1.08	9.39

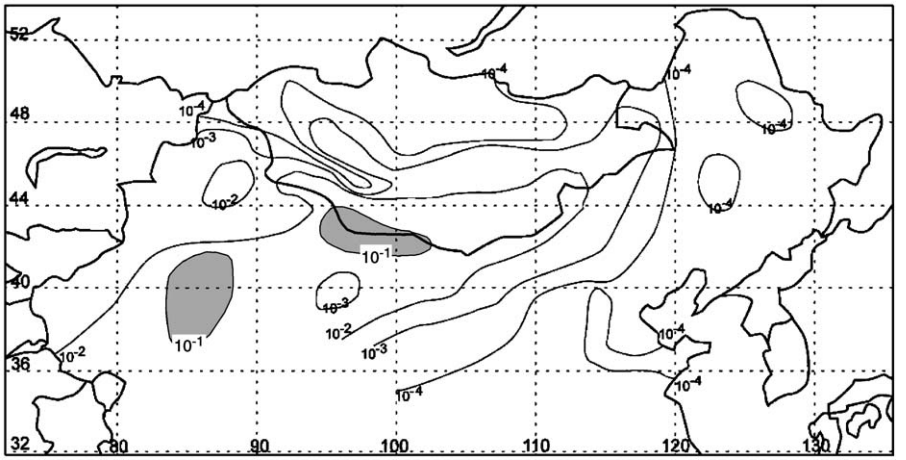

Fig. 2. Annual PM_{10} emission rate in Northern China and Mongolia, Q_{10} ($t\,ha^{-1}\,yr^{-1}$). Two strong emission centers are circled by the contours of $Q_{10} = 10^{-1}\,t\,ha^{-1}\,yr^{-1}$, one is the Taklimakan Desert located in the Tarim Basin while the other is the Central Gobi-desert.

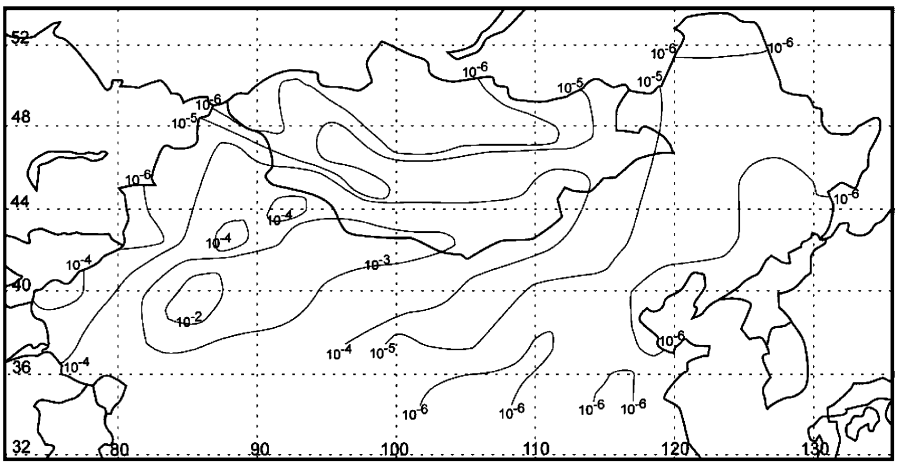

Fig. 3. Annual emission rate of Fe in PM_{10}, Q_{10Fe} ($t\,ha^{-1}\,yr^{-1}$).

becoming deserts and gobi-deserts of Central Asia and the north Tibetan Plateau.

3. Emission inventory of eight elements: Fe, Al, K, Mg, Mn, Na, Ca and Ti

Zheng (1994) published the maps of elemental content in surface soils of PR China, his 1008 sampling points cover the whole dust source area in Northern China. In the maps, totally 56 elements including the eight important geo-chemical elements, Fe, Al, K, Mg, Mn, Na, Ca and Ti, in the horizon A or the upper layer of soil profiles are, respectively, marked with the eight grades of percentage contents. This kind of data is not available for Mongolian soils. Fortunately, the soil classification in both the countries follows the same rules or system by the former USSR Academy of Sciences (Mongolian soil classification: Pisparov, 1959; Chinese soil classification: Xiong and Li, 1990). As Zheng (1994) has concluded that the percentage content of soil elements is mostly correlated with the soil-type and, secondly, the surface soil texture, we again suppose an accordant correlation between the percentage content of an element and the soil types, or surface soil texture, for the whole Mongolian Plateau. In this way, the percentage content of an element in a Mongolian surface soil type is supposed roughly equaling to that of the same soil type (or same surface soil texture in fewer cases) on the Inner-Mongolia Plateau (the south part of the Mongolian Plateau in Chinese side of the border). As examples, Figs. 3–10 show the contour maps of the annual emission rate in dust PM_{10} for the eight elements in the Northern China and Mongolia: Q_{10Fe}, Q_{10Al},

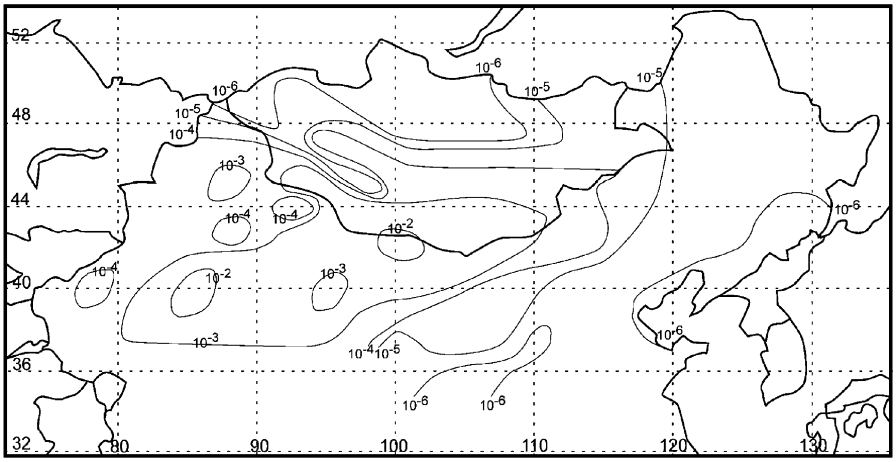

Fig. 4. Annual emission rate of Al in PM_{10}, Q_{10Al} ($t\,ha^{-1}\,yr^{-1}$).

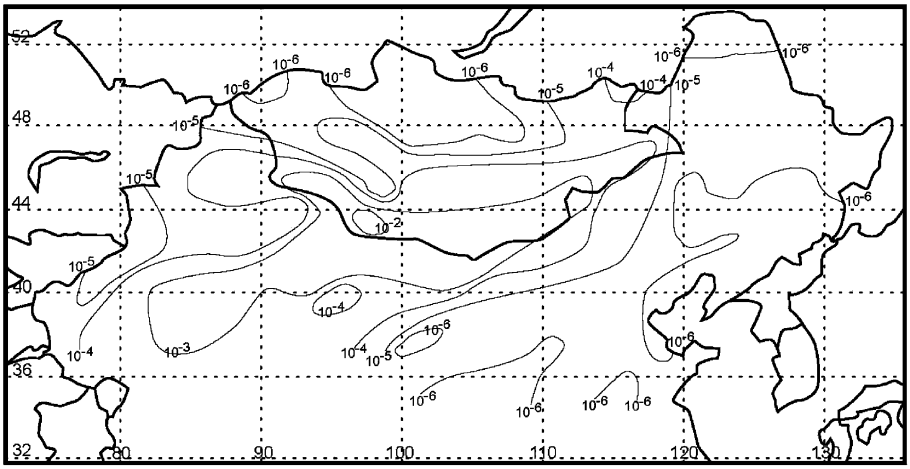

Fig. 5. Annual emission rate of K in PM_{10}, Q_{10K} ($t\,ha^{-1}\,yr^{-1}$).

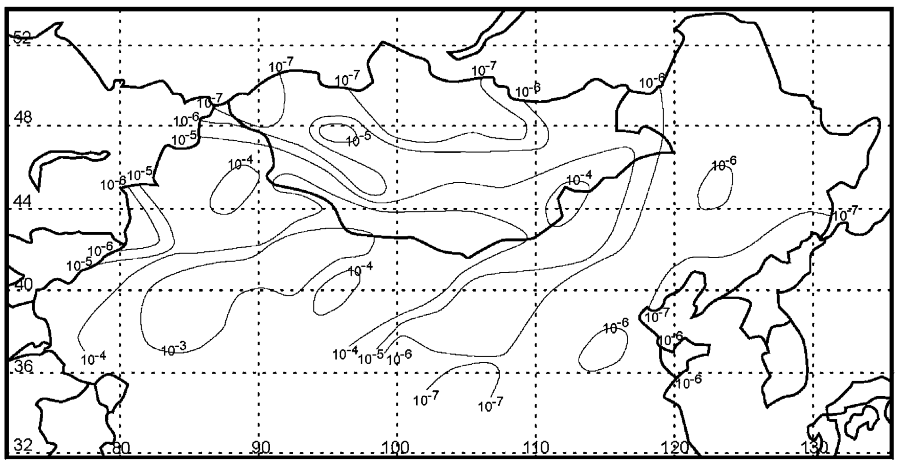

Fig. 6. Annual emission rate of Mg in PM_{10}, Q_{10Mg} ($t\,ha^{-1}\,yr^{-1}$).

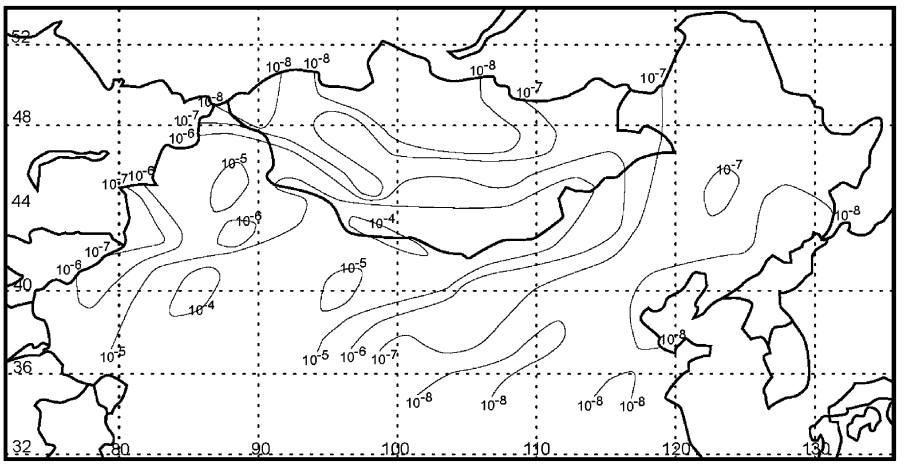

Fig. 7. Annual emission rate of Mn in PM_{10}, Q_{10Mn} ($t\,ha^{-1}\,yr^{-1}$).

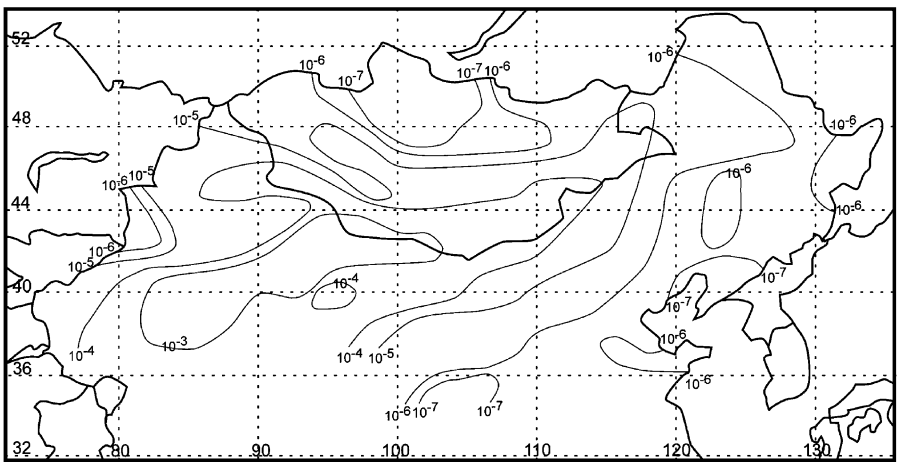

Fig. 8. Annual emission rate of Na in PM_{10}, Q_{10Na} ($t\,ha^{-1}\,yr^{-1}$).

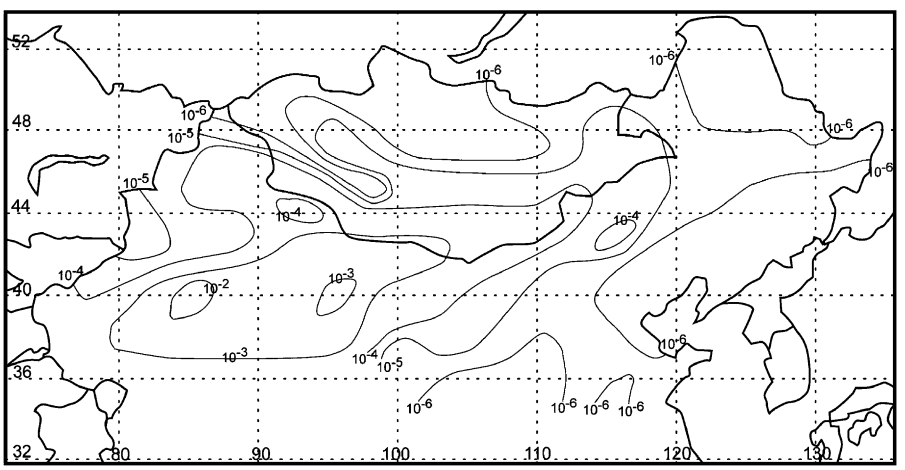

Fig. 9. Annual emission rate of Ca in PM_{10}, Q_{10Ca} ($t\,ha^{-1}\,yr^{-1}$).

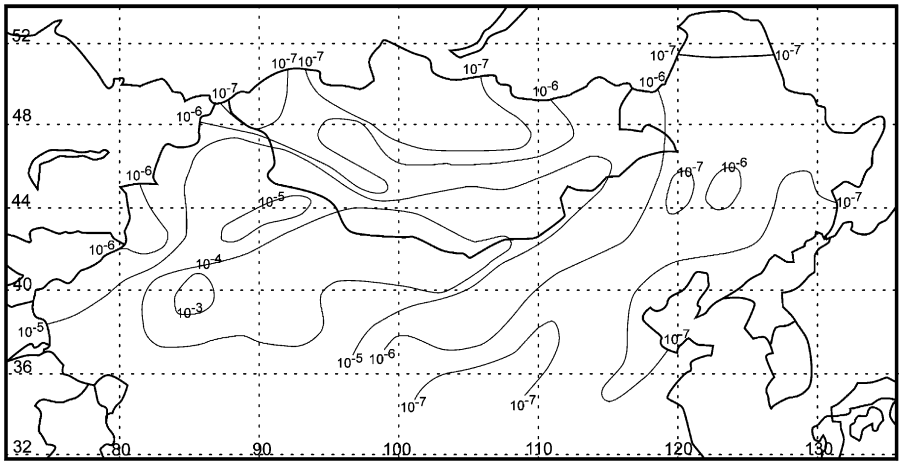

Fig. 10. Annual emission rate of Ti in PM_{10}, Q_{10Ti} ($t\,ha^{-1}\,yr^{-1}$).

Table 2
Mean percentages content of eight elements in surface soils

	Type 1 (Mongolia)[a]	Type 2 (Mongolia)[a]	Type 3 (Mongolia)[a]	Type 1 (China)[b]	Type 2 (China)[b]	Type 3 (China)[b]
Fe (%)	2.02	2.29	2.29	2.16	2.66	2.75
Al (%)	5.33	5.36	5.36	5.63	6.10	5.51
K (%)	2.24	1.94	1.94	2.08	1.80	1.93
Mg (%)	0.50	0.88	0.88	0.65	1.23	1.37
Mn (%)	0.045	0.050	0.050	0.045	0.055	0.069
Na (%)	1.48	1.64	1.64	1.48	1.40	1.52
Ca (%)	1.87	3.16	3.16	2.21	3.81	4.67
Ti (%)	0.28	0.27	0.27	0.29	0.31	0.32

[a]Estimated by corresponding soil types (soil texture) on the Inner-Mongolia Plateau.
[b]Calculated with the maps of elemental contents in surface soils of China by Zheng (1994).

Q_{10K}, Q_{10Mg}, Q_{10Mn}, Q_{10Na}, Q_{10Ca}, and Q_{10Ti}. In each of the 131 grid points, the calculation was with the relationship

$$Q_{10Fe} = \alpha_{Fe} Q_{10}, \quad (1)$$

where α_{Fe} denotes the percentage content of Fe in surface soils, the same for the other elements.

It is interesting to see that all eight contour maps of the elemental emission rates exhibit the same distribution pattern with that of the dust PM_{10} emission rate in Fig. 2. The similarity between the two different kinds of contours comes from the two factors: the percentage element content α varies limitedly in the region, e.g., α_{Fe} ranges between 1% and 6%, while the dust emission rate, both Q_{50} and Q_{10}, changes violently across the region by as much as five scales (Fig. 2). As the soil-types and surface soil texture are relatively uniform in a source type area, a simple method has been used to calculate the elemental emission inventory in the source region of East Asia: in each of the six soil-type areas, multiplying the total PM_{10} or PM_{50} emission with the mean percentage content of the element in surface soils. Table 2 lists the mean percentage content $\bar{\alpha}$ of the eight elements in the six source-type areas, which we calculated with Zheng's (1994) maps. And, Table 3 lists the elemental emission inventory, which we calculated for the dust source region of East Asia. Obviously, the method can also be used for the rest of the 48 elements.

We have compared the total Fe emission in the source region of East Asia, which we calculated, with the total Fe deposition to the North Pacific Ocean, measured and calculated by previous authors (Gao et al., 2001), and found an encouraging agreement. It can be seen from Table 3, the first two rows, that the total Fe emission in East Asia has a maximum in spring and a minimum in summer, and that the total Fe emission in autumn is a little higher than that of winter. On the other hand, according to Gao et al. (2001), the total Fe deposition to the North Pacific Ocean shows exactly the same seasonal variation pattern, totally different from that of all other oceans. The accordance in seasonal variation of the emission and deposition is an evidence that the dust

Table 3
Emission inventories of eight elements in dust source region of East Asia

Total emission	Spring (10^6 ton)	Summer (10^6 ton)	Autumn (10^6 ton)	Winter (10^6 ton)	Annual (10^6 ton)
Fe in PM_{10}	0.16	0.02	0.05	0.04	0.27
Fe in PM_{50}	0.74	0.10	0.27	0.24	1.35
Al in PM_{10}	0.34	0.04	0.11	0.10	0.59
Al in PM_{50}	1.55	0.23	0.56	0.55	2.89
K in PM_{10}	0.11	0.01	0.04	0.03	0.19
K in PM_{50}	0.53	0.08	0.19	0.17	0.97
Mg in PM_{10}	0.07	0.01	0.03	0.02	0.13
Mg in PM_{50}	0.35	0.05	0.13	0.11	0.64
Mn in PM_{10}	0.0037	0.0004	0.0013	0.0010	0.0064
Mn in PM_{50}	0.0176	0.0024	0.0066	0.0052	0.0318
Na in PM_{10}	0.09	0.01	0.03	0.03	0.16
Na in PM_{50}	0.42	0.06	0.15	0.14	0.77
Ca in PM_{10}	0.25	0.03	0.09	0.06	0.43
Ca in PM_{50}	1.18	0.16	0.44	0.35	2.13
Ti in PM_{10}	0.018	0.002	0.006	0.006	0.032
Ti in PM_{50}	0.086	0.012	0.032	0.028	0.158

emission from the sources in East Asia contributes main part of the dust deposition to the North Pacific Ocean. The conclusion seems reasonable if only one thinks about the downwind location of the North Pacific Ocean from the dust source region of East Asia. Further, the total annual Fe deposition to the North Pacific Ocean was estimated to be 3.0×10^6 ton yr^{-1} (Gao et al., 2001), which is compatible in scale with our calculation of the total annual Fe emission from the dust source region of East Asia: 0.27×10^6 ton yr^{-1} (in PM_{10}) and 1.35×10^6 ton yr^{-1} (in PM_{50}). As the Fe deposition data of Gao et al. (2001) are from extrapolation of the in situ aerosol measurements, without any correlation with our calculation method, the scale agreement between their iron (Fe) deposition and our Fe emission seems a strong support for our conclusions.

4. Summary

(1) General feature of the dust source region in East Asia, which consists of deserts and gobi-deserts in Northern China and Southern Mongolia, is described with the contour map of dust PM_{10} emission rate Q_{10}. Also, the emission inventory of PM_{10} and PM_{50}, seasonal and annual, in the source region and its six source type areas is calculated.
(2) The emission rate of the eight important elements of Asian dust, Fe, Al, K, Mg, Mn, Na, Ca and Ti, is calculated in the dust source region of East Asia. The contour maps of the element emission rate all show a similar distribution pattern with that of the PM_{10} emission rate.
(3) The emission inventory of the eight elements in dust PM_{10} and PM_{50}, seasonal and annual, is calculated by multiplying the total emission of dust PM_{10} or PM_{50} in each source-type area with the mean percentage content of the element in surface soils of the source type area.
(4) Comparison of our calculation of Fe emission from the dust source region in East Asia with the iron (Fe) deposition to the North Pacific Ocean, measured and calculated by previous authors, shows good accordance: both exhibit the same seasonal variation pattern and the annual values compatible to each other.

Acknowledgment

I am grateful to the anonymous referee for the valuable comments and suggestions. And, I thank my daughter Mingyue Xuan and daughter-in-law Bonnie Wang for drawing the figures.

References

Choi, J.C., Lee, M., Chun, Y., Kim, J., Oh, S., 2001. Chemical composition and source signature of spring aerosol in Seoul, Korea. Journal of Geophysical Research 106D, 18067–18074.

Gao, Y., Kaufman, Y.J., Tanre, D., Kolber, D., Falkowski, P.G., 2001. Seasonal distributions of aeolian iron fluxes to the global ocean. Geophysical Research Letters 28, 29–32.

Gao, Y., Fan, S., Sarmiento, J.L., 2003. Aeolian iron input to the ocean through precipitation scavenging: a modeling perspective and its implication for natural iron fertilization in the ocean. Journal of Geophysical Research 108D, 4221.

Littmann, T., 1991. Dust storm frequency in Asia: climatic control and variability. International Journal of Climatology 11, 393–412.

Ma, C-J., Tohno, S., Kasahara, M., Hayakawa, S., 2004. The nature of individual solid particles retained in size-resolved raindrops fallen in Asian dust storm event during ACE-Asia. Atmospheric Environment 38, 2951–2964.

Middleton, N., 1991. Dust storms in the Mongolian People's Republic. Journal of Arid Environments 20, 287–297.

Nagoya University, 1995. Yellow Sand (Chinese version). China Construction Press, Beijing.

Pisparov, H., 1959. Mongolian Soils. Science Press (Chinese version), Beijing.

Prospero, J., Ginoux, P., Torres, O., Nicholson, S., Gill, T., 2002. Environmental characterization of global sources of atmospheric soil dust derived from the NIMBUS-7 Total Ozone Mapping Spectrometer (TOMS) absorbing aerosol product. Reviews of Geophysics 40 (1), 1002.

Senaratne, I., Shooter, D., 2004. Elemental composition in source identification of brown haze in Auckland, New Zealand. Atmospheric Environment 38, 3049–3059.

Tazaki, K., Wakimoto, R., Minami, Y., Yamamoto, M., Miyata, K., Sato, K., Saji, I., Chaerun, K., Zhou, G., Morishita, T., Asada, R., Segawa, H., Imanishi, H., Kato, R., Otani, Y., Watanabe, T., 2004. Transport of carbon-bearing dusts from Iraq to Japan during Iraq's War. Atmospheric Environment 38, 2091–2109.

Topping, D., Coe, H., McFiggans, G., Burgess, R., Allan, J., Alfarra, M.R., Bower, K., Choularton, T.W., Decesari, S., Facchini, M.C., 2004. Aerosol chemical characteristics from sampling conducted on the Island of Jeju, Korea during ACE Asia. Atmospheric Environment 38, 2111–2123.

Xiong, Y., Li, Q., 1990. Soil of China. Science Press, Beijing.

Xuan, J., 1999. Dust emission factors for environment of Northern China. Atmospheric Environment 33, 1767–1776.

Xuan, J., Sokolik, I., 2002. Characterization of sources and emission rates of mineral dust in Northern China. Atmospheric Environment 36, 4863–4876.

Xuan, J., Liu, G., Du, K., 2000. Dust emission inventory in Northern China. Atmospheric Environment 34, 4565–4570.

Xuan, J., Sokolik, I., Hao, J., Guo, F., Mao, H., Yang, G., 2004. Identification and characterization of sources of atmospheric dust in East Asia. Atmospheric Environment 38 (36), 6239–6252.

Zheng, C. (Ed.), 1994, Atlas of Soil Environmental Background Value in the People's Republic of China. China Environmental Science Press, Beijing.